

# OLCI Level 2

## Algorithm Theoretical Basis Document

### **Photosynthetically Active Radiation**

DOCUMENT REF: S3-L2-SD-03-C12-ARG-ATBD  
DELIVERABLE REF: SD-03-C  
VERSION: 1.2

## Document Signature Table

	Name	Function	Company	Signature	Date
<b>Prepared</b>	S. Lavender	Project Manager	ARGANS		
<b>Approved</b>	O. Fanton d'Andon	OLCI Coordinator	ACRI-ST		
<b>Released</b>	S. Lavender	Project Manager	ARGANS		

## Change record

Issue	Date	Description	Change pages
<b>1.0</b>	24/08/2009	Initial version	
<b>1.1</b>	18/01/2010	Corrected units for PAR – from $\mu\text{W}/\text{cm}^2/\mu\text{m}$ to $\text{mW}/\text{cm}^2/\mu\text{m}$	9
<b>1.2</b>	11/04/2010	Minor updates for CDR: added comment on MERIS iPAR product	



**SENTINEL-3 OPTICAL PRODUCTS AND ALGORITHM  
DEFINITION**

**OLCI Level 2 Algorithm Theoretical Basis Document  
Photosynthetically Active Radiation**

Ref: S3-L2-SD-03-C12-ARG-ATBD  
Issue: 1.2  
Date: 11/04/10  
Page 3 of 15

## Distribution List

Organisation	To	Nb. of copies
ESA	P. Goryl	
EUMETSAT	Hilary Wilson, Anne O'Carroll	
S3 Optical team	All OLCI team	

## Table of Contents

1. INTRODUCTION .....	6
1.1 Acronyms and Abbreviations .....	6
1.2 Symbols .....	6
<b>1.3</b> Purpose and Scope .....	7
1.4 Algorithm Identification .....	7
2. ALGORITHM OVERVIEW .....	7
2.1 Objectives .....	8
3. ALGORITHM DESCRIPTION .....	8
3.1 Theoretical Description .....	8
3.2 Algorithm Validation .....	10
3.1 Practical consideration .....	11
4. ASSUMPTIONS AND LIMITATIONS .....	13
5. INPUT DATA .....	14
6. ERROR BUDGET .....	14
7. REFERENCES .....	15

	<p style="text-align: center;"><b>SENTINEL-3 OPTICAL PRODUCTS AND ALGORITHM DEFINITION</b></p> <p style="text-align: center;"><b>OLCI Level 2 Algorithm Theoretical Basis Document Photosynthetically Active Radiation</b></p>	<p>Ref: S3-L2-SD-03-C12-ARG-ATBD Issue: 1.2 Date: 11/04/10 Page 5 of 15</p>
---	--	---

## List of Figures

Figure 1: PAR from three sensors, and also including SeaWiFS\_MER (application of the reformulated MERIS approach, Frouin 2008, to SeaWiFS), compared to a) AMT 12 and b) AMT 13 in situ PAR. Source: GlobColour PAR report (Lavender 2008). ..... 12

Figure 2: Regression plots of in situ AMT PAR with PAR estimated by each sensor using the MERIS PAR (Frouin, 2008) algorithm. Included also, is the NASA SeaWiFS operational PAR product regressed with AMT 13. Source: GlobColour PAR report (Lavender 2008). ..... 13

## 1. INTRODUCTION

### 1.1 Acronyms and Abbreviations

AMT	Atlantic Meridional Transect
ATBD	Algorithm Theoretical Basis Document
LUT	Look Up Table
MERIS	Medium Resolution Imaging Spectrometer
MODIS	Moderate Resolution Imaging Spectrometer
OLCI	Ocean Land Colour Imager
PAR	Photosynthetically Active Radiation
SeaWiFS	Sea-viewing Field-of-view Spectrometer
TOA	Top of Atmosphere

### 1.2 Symbols

Symbol	definition	Dimension / units
<b>Geometry, wavelengths</b>		
$\lambda$	Wavelength	nm
$\theta_s$	Sun zenith angle ( $\mu_s = \cos(\theta_s)$ )	degrees
$\theta_v$	Satellite viewing angle ( $\mu_v = \cos(\theta_v)$ )	degrees
<b>Atmospheric properties</b>		
$P_{aer}$	Aerosol phase function	
$P_{mol}$	Molecular phase function	
$T_d(\lambda, \theta)$	Diffuse transmittance for angle $\theta$	dimensionless
	$T_d(\lambda, \theta) = L_i(\lambda, \theta_s, \theta_v, \Delta\phi) / L_{o+}(\lambda, \theta_s, \theta_v, \Delta\phi)$	
$T_g(\lambda, \theta)$	Gaseous transmission	
$\rho(\lambda, \theta_s, \theta_v, \Delta\phi)$	Reflectance ( $\pi L / F_0 \mu_s$ )	dimensionless

where the product  $\pi.L$  is the TOA upwelling irradiance if upwelling radiances are equal to  $L(\lambda, \theta_s, \theta_v, \Delta\phi)$ , for any values of  $\theta_v$  within  $0-\pi/2$  and any  $\Delta\phi$  within  $0-2\pi$ .

Subscripts are

a: Intrinsic atmospheric reflectance

cs: cloud/surface layer

gc: gas corrected

dimensionless

$\tau_{aer}$	Optical thicknesses of aerosols
$\tau_{mol}$	Optical thicknesses of molecules
$\omega_{aer}$	Single scattering albedo of aerosols

### 1.3 Purpose and Scope

Photosynthetically Active Radiation (PAR) reaching the ocean surface is defined as the quantum energy flux from the Sun in the spectral range 400-700 nm; units are Einstein/m<sup>2</sup>/day. PAR is essential for the carbon-cycle modellers to convert the measured chlorophyll concentration into an estimate of ocean productivity, and hence of carbon sequestration.

### 1.4 Algorithm Identification

This algorithm is identified under reference “SD-03-C12” in the Sentinel-3 OLCI documentation.

## 2. ALGORITHM OVERVIEW

The MERIS PAR product was adapted to the operational context of MERIS by Aiken and Moore (1997), based on the Gregg and Carder (1990) model, through the creation of a look-up table (LUT). It's defined as the number of quanta reaching the water surface in the 400 nm to 700 nm spectral window per surface unit and per time unit, see Equation 1, Bouvet (2006):

$$PAR = 1/hc \int_{400nm}^{700nm} \lambda E_d(\lambda) d\lambda \quad (\text{Eq 1})$$

where h and c are respectively the Planck constant and the speed of light in a vacuum and  $E_d$  is the downwelling irradiance just above the sea surface.

The MERIS PAR product is an instantaneous PAR (iPAR) that was developed alongside the chlorophyll fluorescence (Aiken and Moore, 1997) product and can only be calculated for clear skies. Although it's believed that iPAR is very useful for Net Primary Production (NPP) and other ecosystem models, many models require a daily time step and thus a daily PAR product is more

	<b>SENTINEL-3 OPTICAL PRODUCTS AND ALGORITHM DEFINITION</b>  <b>OLCI Level 2 Algorithm Theoretical Basis Document Photosynthetically Active Radiation</b>	Ref: S3-L2-SD-03-C12-ARG-ATBD Issue: 1.2 Date: 11/04/10 Page 8 of 15
---	---	---

desirable. Therefore, the Frouin et al. (2005) approach that's applied to MODIS and SeaWiFS and lead into the GlobColour multi-sensor merged PAR product has been included. This produces an average daily (24 hour) flux and is calculated for all pixels.

## 2.1 Objectives

The atmosphere and surface are modelled as a 2-layer system. The first layer contains molecules and aerosols and is located above the second layer, the cloud/surface layer. The OLCI reflectances are corrected for gaseous absorption and then for molecular and aerosol scattering, which yields the instantaneous albedo of the cloud/surface layer in the PAR interval,  $A$ . This albedo is then used to compute instantaneous PAR, and finally, daily PAR is obtained by integrating instantaneous PAR from sunrise to sunset. The dependence of  $A$  on sun zenith angle is taken into account, but atmospheric conditions are assumed to be constant during the day and to correspond to the satellite observation.

## 3. ALGORITHM DESCRIPTION

### 3.1 Theoretical Description

Frouin et al. (2005) estimate daily PAR reaching the ocean surface using a parallel-plane theory and assume a decoupling of the effects of clouds and clear sky. Consequently, the algorithm doesn't have to distinguish between clear and cloudy regions within a pixel. The solar flux reaching the ocean surface is then given by Equation 2 (Frouin, 2005).

$$E = E_{clear} (1 - A)(1 - A_s)^{-1}(1 - S_\alpha A)^{-1} \quad (\text{Eq 2})$$

Where is where  $A_s$  is the albedo of the ocean surface and  $E_{clear}$  is the solar flux that would reach the surface if the cloud/surface system were non reflecting and non-absorbing. To compute  $E$ ,  $A$  is expressed as a function of the satellite measured radiance in the PAR spectral range and the reflectance of the cloud/surface layer,  $\rho_{cs}(\lambda)$ , is obtained from the gas absorption corrected top of atmosphere reflectance,  $\rho_{gc}(\lambda)$ , following Equation 3 (Tanré et al., 1979) assuming isotropy of the cloud/surface layer system.

$$\rho_{cs}(\lambda) = \left( \rho_{gc}(\lambda) - \rho_a(\lambda) \right) \left[ T_d(\theta_s, \lambda) T_d(\theta_v, \lambda) + S_a(\lambda) \left( \rho_{gc}(\lambda) - \rho_a(\lambda) \right) \right]^{-1} \quad (\text{Eq 3})$$

$\rho_a(\lambda)$ , the aerosol reflectance, is modelled using the quasi single-scattering approximation, Equation 4 (Frouin, 2005). From this point onwards, the variation with wavelength ( $\lambda$ ) has been dropped for clarity.

$$\rho_a = (\tau_{mol} P_{mol} + \omega_{aer} \tau_{aer} P_{aer}) [4\mu_s \mu_v]^{-1} \quad (\text{Eq 4})$$

The terms include the optical thicknesses of molecules and aerosols,  $\tau_{mol}$  &  $\tau_{aer}$ , their respective phase functions,  $P_{mol}$  &  $P_{aer}$ , and the single scattering albedo of aerosols,  $\omega_{aer}$ . The molecular phase function is calculated according to Equation 5 (Frouin, 2008).

$$P_{mol} = \frac{(2.0 * (1.0 - del) * 0.75 * (1.0 + \cos 2X) + 3.0 * del)}{(2.0 + del)} \quad (\text{Eq 5})$$

$$\cos 2X = \cos X * \cos X \quad (\text{Eq 6})$$

$$Chi = ACOSD(\cos X) \quad (\text{Eq 7})$$

$$\cos X = -(\mu_s \mu_v) + (\sin \theta_s * \sin \theta_v * \cos \Delta \phi) \quad (\text{Eq 8})$$

Where  $del = 0.0095$ . The diffuse transmittance,  $T_d(\theta)$ , and spherical albedo,  $S_a$ , are computed using analytical formulas developed by Tanré et al. (1979), see Equations 9 and 10 (Frouin, 2005).

$$T_d(\theta) = \exp \left[ \frac{-(\tau_{mol} + \tau_{aer})}{\mu \theta} \right] \exp \left[ \frac{(0.52 \tau_{mol} + B \tau_{aer})}{\mu \theta} \right] \quad (\text{Eq 9})$$

Where  $B = 0.5(1.0 + Asym)$ , and  $Asym = 0.6666667$  (Frouin, 2008).

$$S_a = (0.92 \tau_{mol} + G \tau_{aer}) \exp[-(\tau_{mol} + \tau_{aer})] \quad (\text{Eq 10})$$

Where  $G = 1.0 - Asym$  and  $\theta$  is either the sun or sensor zenith angle. The aerosol optical thickness in band  $i$  is obtained from the optical thickness in OLCI band 16 (865 nm),  $\tau_{aerref}$ , and the Angstrom coefficient ( $\alpha$ ), between 665 (OLCI band 8) and 865nm, see Equation 11 (Frouin, 2005).

$$\tau_{aer} = \tau_{aerref} \left( \frac{\lambda_{ref}}{\lambda_i} \right)^\alpha \quad (\text{Eq 11})$$

An estimate of daily PAR,  $\langle E \rangle_{day}$ , is obtained by integrating Equation 2 over the length of the day, see Equation 12 (Frouin, 2005).

$$\langle E \rangle_{day} = \langle E_0 \rangle \int \{ \mu_s \langle T_g \rangle \langle T_d \rangle [1 - \langle A \rangle] [1 - \langle A_s \rangle]^{-1} [1 - \langle S_a \rangle \langle A \rangle]^{-1} \} dt \quad (\text{Eq 12})$$

Where,  $\langle \rangle$  symbolizes average value over the PAR range,  $T_g$  is the gaseous transmission.

$$\langle A \rangle = \frac{\langle \rho_{cs}(\lambda) \rangle}{\langle E_0 \rangle} \quad (\text{Eq 13})$$

$$\langle A_s \rangle = \langle T_{dir} \rangle \langle T_d \rangle^{-1} \left[ \frac{0.5}{1.1[\mu_s]^{1.4+0.15}} \right] + 0.07 \langle T_{dir} \rangle \langle T_d \rangle^{-1} \quad (\text{Eq 14})$$

$$T_{dir} = \exp \left[ \frac{-(\tau_{mol} + \tau_{aer})}{\mu_s} \right] \quad (\text{Eq 15})$$

$$T_{dif} = 1 - T_{dir} \quad (\text{Eq 16})$$

Finally, the individual daily PAR estimates, obtained in units of  $\text{mW}/\text{cm}^2/\mu\text{m}$ , are converted into units of  $\text{Einstein}/\text{m}^2/\text{day}$  and can then be spatially and temporally averaged into global (Level) 3 daily, weekly and monthly products. The factor required to convert units of  $\text{mW}/\text{cm}^2/\mu\text{m}$  to units of  $\text{Einstein}/\text{m}^2/\text{day}$  is equal to 1.193 to an inaccuracy of a few percent regardless of meteorological conditions (Kirk, 1994, pp. 4-8.). In middle and high latitudes, several daily estimates may be obtained over the same target during the same day, increasing product accuracy.

### 3.2 Algorithm Validation

Validation of the MERIS, MODIS and SeaWiFS PAR products occurred within a GlobColour activity (Lavender 2008). The satellite PAR products were compared to in situ Atlantic Meridional Transect (AMT) cruise PAR on a time series basis and down the latitudinal track, respectively, see Figure 1. The overall trend in PAR reflects latitudinal variability while the high frequency variability reflects local cloud conditions on the particular day being sampled;

	<p style="text-align: center;"><b>SENTINEL-3 OPTICAL PRODUCTS AND ALGORITHM DEFINITION</b></p> <p style="text-align: center;"><b>OLCI Level 2 Algorithm Theoretical Basis Document Photosynthetically Active Radiation</b></p>	<p>Ref: S3-L2-SD-03-C12-ARG-ATBD Issue: 1.2 Date: 11/04/10 Page 11 of 15</p>
---	--	--

it should be remembered that neither the in situ or satellite products are the truth, but in these comparisons the in situ magnitude will be considered as the best representation of the truth.

There were not as many MERIS matchups to the AMT sample dates as there are for SeaWiFS and MODIS. For AMT 12 there were 10 matching points and for AMT 13 there were 9 matching points. Figure 2 shows the correlation of the satellite match-ups with the in situ data; positive and significant linear correlations of 0.896 (AMT 12) and 0.863 (AMT 13) for MERIS. However, the correlations only indicate that the predicted magnitudes rather than variability is correct. The difficult question to answer with this preliminary validation is whether the in situ (AMT) high frequency variability is real / needed for the modellers or an artefact of the in situ data collection method.

### 3.1 Practical consideration

For Frouin (2005), a monthly climatology for  $\tau_{aerref}$  (865 nm for SeaWiFS) and  $\alpha$  was based on three years of SeaWiFS data (1997-2000) since aerosol properties cannot be determined when the pixel is cloudy. This was justified because, in general, aerosol effects on E are secondary compared to cloud or  $\theta_s$  effects. For Frouin (2008) an external Look Up Table (LUT) called "meris\_aerosol\_par.dat" was used.

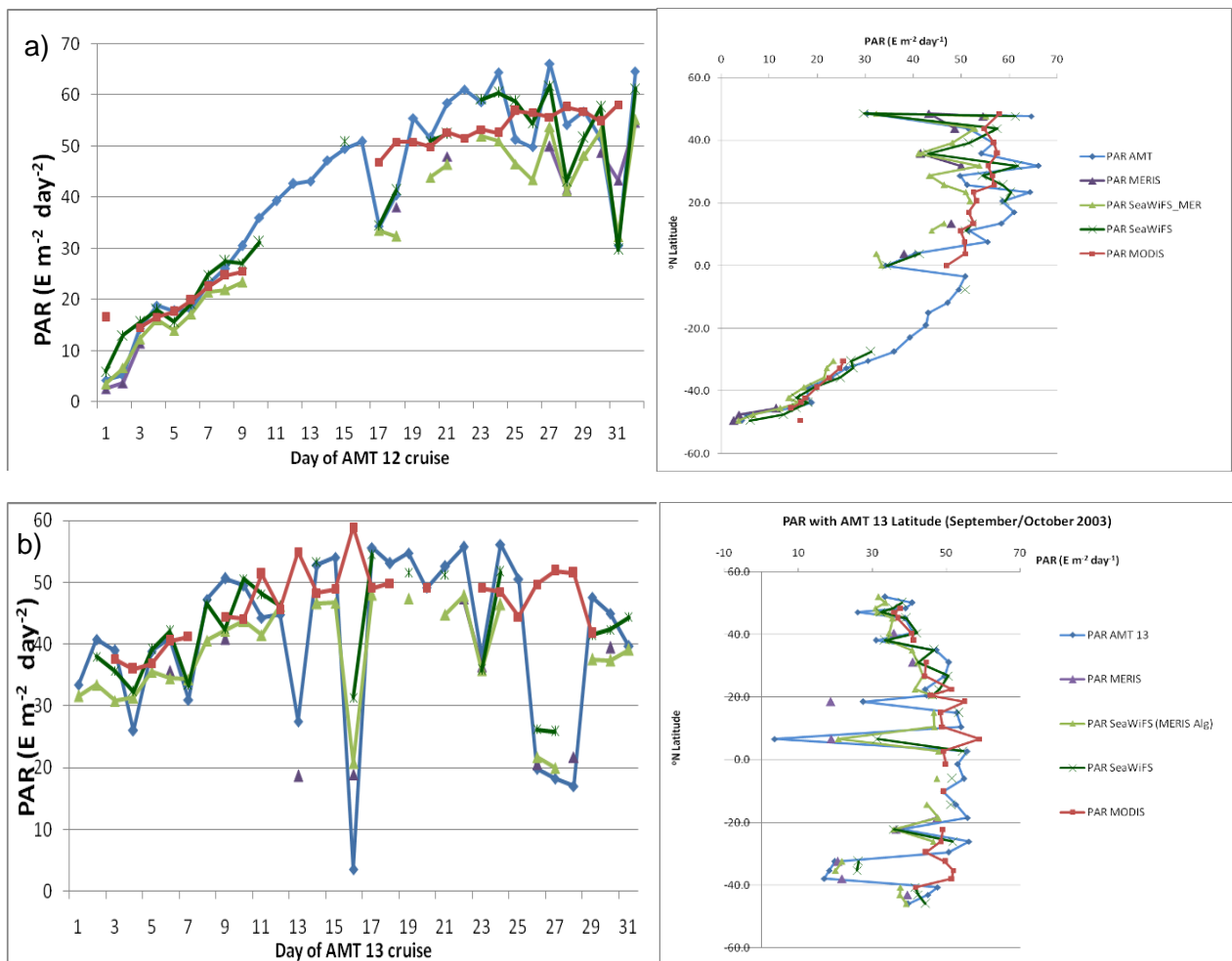


Figure 1: PAR from three sensors, and also including SeaWiFS\_MER (application of the reformulated MERIS approach, Frouin 2008, to SeaWiFS), compared to a) AMT 12 and b) AMT 13 in situ PAR. Source: GlobColour PAR report (Lavender 2008).

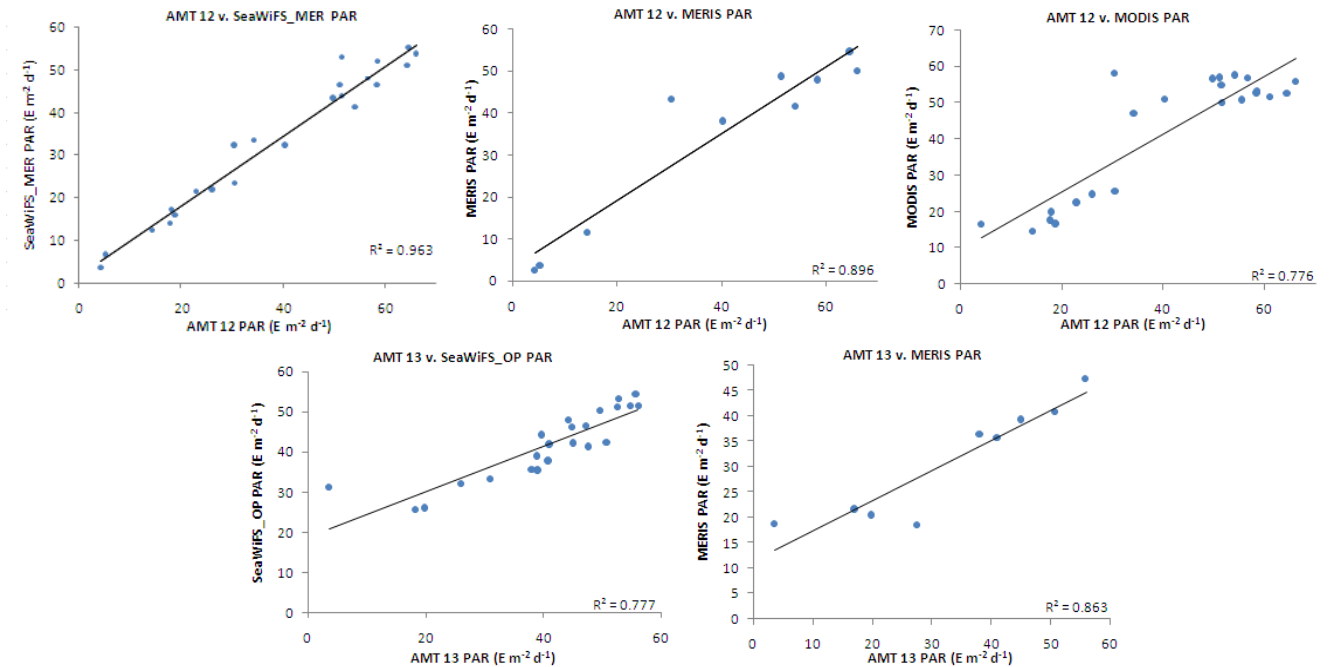


Figure 2: Regression plots of in situ AMT PAR with PAR estimated by each sensor using the MERIS PAR (Frouin, 2008) algorithm. Included also, is the NASA SeaWiFS operational PAR product regressed with AMT 13. Source: GlobColour PAR report (Lavender 2008).

#### 4. ASSUMPTIONS AND LIMITATIONS

The quasi single-scattering approximation is inaccurate at large zenith angles, but acceptable for the OLCI sun zenith angles (less than 75 degrees).

The cloud/surface system is assumed to be stable during the day and to correspond to the OLCI observation. This assumption is crude, and PAR accuracy will be degraded in regions where clouds exhibit strong diurnal variability.

Ideally, the PAR product should be produced after the atmospheric correction has been performed so that outputs of the atmospheric correction are available.

	<p style="text-align: center;"><b>SENTINEL-3 OPTICAL PRODUCTS AND ALGORITHM DEFINITION</b></p> <p style="text-align: center;"><b>OLCI Level 2 Algorithm Theoretical Basis Document Photosynthetically Active Radiation</b></p>	<p>Ref: S3-L2-SD-03-C12-ARG-ATBD Issue: 1.2 Date: 11/04/10 Page 14 of 15</p>
---	--	--

The MERIS iPAR may be required. As the MERIS algorithm is relatively straightforward to implement this could be implemented alongside the current daily PAR algorithm and 2 products produced.

## 5. INPUT DATA

### Input from Level1:

Geometry including illumination and viewing zenith and azimuth angles:  $\theta_s$  [degrees],  $\theta_v$  [degrees] and  $\Delta\phi$  [degrees]

TOA gas corrected sensor reflectance:  $\rho_{gc}(\lambda)$  [dimensionless]

### Input from earlier processing steps:

Gaseous transmission:  $T_g$  [dimensionless]

Optical thickness for molecules:  $\tau_{mol}$  [dimensionless]

**Input from LUT that provides the following based on Chi (Eq 6) and Angstrom (665,865)\*:**

Optical thickness for aerosols:  $\tau_{aer16}$  [dimensionless]

Phase function for aerosols:  $P_{aer}$  [dimensionless]

Single scattering albedo of aerosols:  $\omega_{aer}$  [dimensionless]

Wavelength varying Angstrom coefficient:  $\alpha$  [dimensionless]

\* Based on aerosol model #5 (Maritime RH=90%) = 0.197490 (Frouin, 2008)

## 6. ERROR BUDGET

An error model will (ideally) be based on probability density functions (PDFs) provided for the input variables ( $\theta_s$ ,  $\theta_v$ ,  $\Delta\phi$ ,  $\rho_{gc}(\lambda)$ ,  $T_g$  and  $\tau_{mol}$ ), which will be propagated through the PAR

	<p style="text-align: center;"><b>SENTINEL-3 OPTICAL PRODUCTS AND ALGORITHM DEFINITION</b></p> <p style="text-align: center;"><b>OLCI Level 2 Algorithm Theoretical Basis Document Photosynthetically Active Radiation</b></p>	<p>Ref: S3-L2-SD-03-C12-ARG-ATBD Issue: 1.2 Date: 11/04/10 Page 15 of 15</p>
---	--	--

equations (model) to obtain an output PDF for PAR. An alternative is a sensitivity analysis where the input variables are varied by  $\pm 5\%$  and the variation in the out PAR analysed.

## 7. REFERENCES

Aiken J. and Moore, G. 1997. Photosynthetic Available Radiation, MERIS ATBD 2.18, version 5 Dec 1997

Bouvet, M. 2006. MERIS Photosynthetically Available Radiation: a product quality assessment. Proceedings of the Second Working Meeting on MERIS and AATSR Calibration and Geophysical Validation (MAVT-2006), ESRIN, Frascati, Italy. Available at [http://envisat.esa.int/workshops/mavt\\_2006/papers/56\\_bouve.pdf](http://envisat.esa.int/workshops/mavt_2006/papers/56_bouve.pdf)

Frouin, R., Franz, B. and Wang, M. 2005. Algorithm to estimate PAR from SeaWiFS data. Version 1.2 – documentation. Available at [http://oceancolor.gsfc.nasa.gov/DOCS/seawifs\\_par\\_wfigs.pdf](http://oceancolor.gsfc.nasa.gov/DOCS/seawifs_par_wfigs.pdf)

Frouin, R. 2008. Software provided to perform the PAR calculation for MERIS: Calc\_PAR\_MERIS version 1.5.

Gregg, W.W. and Carder, K.L. 1990. A simple spectral solar irradiance model for cloudless marine atmospheres. *Limnology and Oceanography*, 35(8), 1657.

Lavender, S.J. 2008. Prototyping a GlobColour merged PAR product, GlobColour PAR Final Report, GC-TN-ARG-PAR-01, Version 1.2, 25 pp.

Kirk, J. T. O., 1994: Light and photosynthesis in aquatic ecosystems, 2nd edition, Cambridge University Press, 509 pp.

Tanre, D., M. Herman, P.-Y. Deschamps, and A. De Lefte, 1979: Atmospheric modeling for Space measurements of ground reflectances, including bi-directional properties. *Appl. Optics*, 18, 21,3587-21,3597.